

## CHAPTER V

### OPTIMIZING THE SACRIFICIAL LAYER ELECTROPHORETIC DEPOSITION TECHNIQUE BY USING DIFFERENT POLYMERS

#### Chapter Overview

The liberation of a nanoparticle film in the sacrificial layer electrophoretic deposition (SLED) process is influenced by the interaction of the film with the underlying polymer and its solvent. We attempted to minimize direct effects of the solvent by choosing solvents in which the nanoparticles were insoluble. Still, the motion of polymer chains dissolving in the sacrificial layer can disrupt the nanoparticle film above it. We speculated that the extent to which polymer chain motion disrupts the film is related to the size of the polymer. In this chapter, we describe our findings on the effect that polymer size has on the resulting nanoparticle films, established using two different polymers and two different polymer size regimes. We begin with a primer on how polymer size is calculated and how the size is a function of the solvent environment around the polymer. Subsequently, we review recent literature, which reports that the size of a polymer also fluctuates with its concentration in solution. We conclude by describing how the nanoparticle film liberation was modified to produce free-standing films with macroscopic dimensions.

#### 5.1 Polymer Chains: A Primer on Solvent Interaction and Size

The physical space occupied by a given polymer chain depends strongly on the solvent environment of the polymer. Linear polymer chains in solution are considered to occupy an elliptical shape, accounting for rotational degrees of freedom [56]. One measure of the polymer chain's effective size is its radius of gyration ( $R_g$ ). Radius of gyration of a chain is defined as the root-mean-square distance of the chain units (monomers) from their center of gravity. The  $R_g$  of a polymer is related to its end-to-end length ( $r$ ) by the relationship

$$R_g^2 = (1/6) r^2 \quad (5.1)$$

for randomly oriented coils [57]. The end-to-end length depends on the conformation of the chain (Figure 5-1). Chain conformation behavior is a thermodynamic effect, contingent on whether the interaction between a monomer and a solvent molecule is energetically favorable.

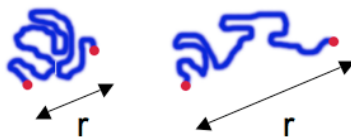


Figure 5-1. Simplified 2-D representation of a polymer chain, whose end-to-end length ( $r$ ) depends on the chain's conformation.

There are three polymer-solvent interaction regimes, which we describe here. (1) In a poor solvent the polymer chain is “balled up” as monomer-monomer interaction is favored over monomer-solvent interaction. (2) In a good solvent the polymer chain resides in an expanded position because of favorable monomer-solvent interaction. (3) In a theta solvent the polymer chain assumes a random coil behavior, wherein it appears to not distinguish between solvent molecules and other monomers with which it is in contact. The free energy of monomer-monomer interaction is balanced by the free energy of monomer-solvent interaction. The theta condition is satisfied for a given polymer-solvent pair at a particular temperature known as the theta temperature. Theta conditions are preferable for the study of polymers because the measured properties generally are independent of the solvent. In a theta solvent, the  $R_g$  of a given polymer is related to the molecular weight ( $M_w$ , weight-average) by the relationship

$$(R_g / M_w^{1/2}) = C \quad (5.2)$$

where  $C$  is a material-specific constant. For example, the value of the constant for polystyrene is  $0.28 \text{ \AA mol}^{1/2} \text{ g}^{-1/2}$  [56].

As a brief aside, neutron scattering experiments have shown that polymers in the solid state have the same values of  $(R_g / M_w^{1/2})$  constants as their counterparts dissolved in theta

solvent. These findings corroborate the description of the theta condition, in which the polymer cannot distinguish between solvent molecules and neighboring polymers.

## 5.2 Changes in Polymer Size as a Solid Polymer Dissolves

In our sacrificial layer experiments, the polymer is a solid before it is dissolved to liberate the nanoparticle film. Therefore, we are interested in what happens to the solid polymer when it is introduced to its solvent. We start with a qualitative description of the process.

When a polymer is below its glass transition temperature (which is the case for our experiments at room temperature), solvent first wets the polymer and then diffuses, relatively slowly, into the space between the polymer chains. Swelling occurs. A moving boundary between swollen and non-swollen material forms, and stresses at the boundary may cause the polymer to fracture. Finally, polymer chains diffuse out of the high-concentration collection of chains and are dissolved [56].

In the literature, molecular dynamics has been used to study this process quantitatively. The  $R_g$  value for polymer chains in a solvent is a function of the polymer-solvent interaction energy (as stated in the previous section) and of the polymer concentration, as a recent study reports [58]. Figure 5-2 shows the relationship between these factors. For a polymer in a good solvent, we note that the  $R_g$  value increases as the concentration decreases (Table 5-1). This is a reasonable assertion, since the increase in available solvent volume allows the chains to expand.

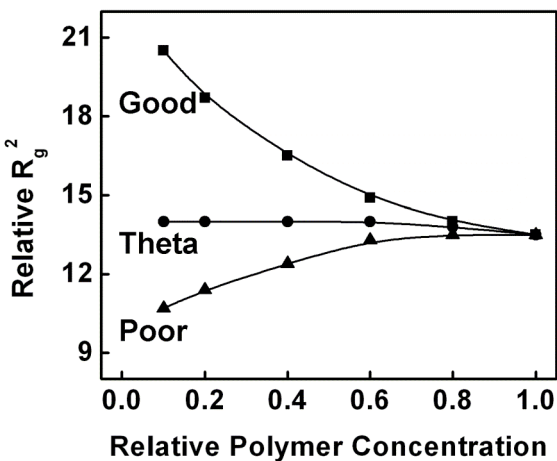


Figure 5-2. Square of radius of gyration plotted against polymer concentration for good, theta, and poor solvent conditions. Calculations reproduced from [58].

Table 5-1. Change in a polymer's radius of gyration as the polymer concentration decreases. Calculated from Figure 5-2 for a polymer in a good solvent.

Relative Polymer Concentration	Change in $R_g$
1 (starting)	—
0.75	+ 2.6%
0.50	+ 7.2%
0.25	+ 15.5%
0.10	+ 23.2%

### 5.3 Polymer Chain Attached to Nanoparticle Film

Now let us consider a nanoparticle film attached to a polymer film, in a solvent-free environment (Figure 5-3). We can calculate the  $R_g$  of the constituent polymer chain from (5.2) since that relationship is valid for both solid polymers and polymers in a theta solvent. Using the  $R_g$  value, we can calculate the end-to-end length of the polymer using (5.1). Knowing this initial value of end-to-end length ( $r_0$ ), we can estimate the number of nanoparticles attached to each chain.

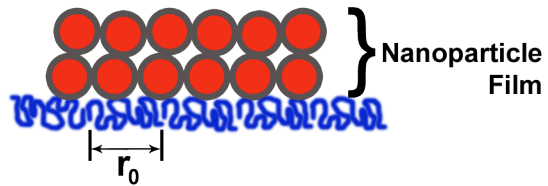


Figure 5-3. Schematic representation of a nanoparticle film atop a polymer layer, in which the polymer chain has an end-to-end length of  $r_0$ .

When the polymer-nanoparticle assembly is placed in a good solvent for the polymer, the solvent infiltrates the polymer and causes it to swell. As polymer begins to diffuse away from the nanoparticle interface, the local concentration of polymer chains decreases, facilitating a further increase in the chain size, as detailed in Table 5-1. The probable consequence of this size increase for the nanoparticle film is illustrated in Figure 5-4. If a single polymer chain is large enough to be attached to multiple adjoining nanoparticles, expansion of the chain can separate the nanoparticles from each other. If the polymer chain is smaller than a nanoparticle, then only the chains that span nanoparticle-nanoparticle boundaries are likely to induce damage of the nanoparticle assembly with their expansion. Therefore, we can expect the sacrificial layer process to yield larger areas of nanoparticle film as the molecular weight of the sacrificial polymer is decreased.

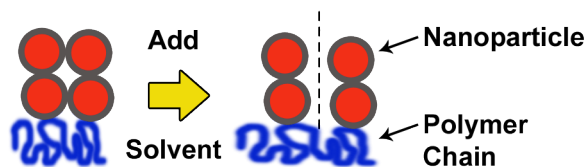


Figure 5-4. If a polymer chain is larger than the nanoparticles attached to it, expansion of the chain in solvent can break apart the nanoparticle assembly.

#### 5.4 Sacrificial Layer Experiments Using Different Polymers

We used three polymers in the investigation of the SLED technique: polystyrene with two different molecular weights ( $M_w = 212,000$  and  $7,200$ , designated as PS-212 and PS-7, respectively) and poly(lactic-co-glycolic acid) with  $M_w = 9,700$  (designated as PLGA). Table 5-2

displays the radii of gyration and end-to-end lengths of these polymers before solvent is introduced. Compared to the iron oxide nanoparticles used in this study (total diameter ~17 nm), a PS-212 chain is larger than the nanoparticles, while chains of PS-7 and PLGA are smaller than the nanoparticles.

Table 5-2. Radius of gyration and end-to-end length of the polymers used in this study.

Polymer	Radius of Gyration	End-to-End Length ( $r_0$ )
PS-212	12.9 nm	31.6 nm
PS-7	2.4 nm	5.8 nm
PLGA	3.3 nm	8.2 nm

The sacrificial polymer layers were spun cast from either toluene or chloroform. For the nanoparticle film liberation, we ruled out the use of toluene to dissolve the polymer because toluene is also an excellent solvent for the nanoparticles. During initial trials with chloroform to liberate the nanoparticle film, we observed that the nanoparticles were weakly soluble in chloroform. Thus, to dissolve the polymer layer, we needed to use a solvent different from those used to cast the layer. Acetone was selected because it is a good solvent for all the polymers and because it does not dissolve the nanoparticles. (Previously, acetone was used to precipitate the synthesized iron oxide nanoparticles out of the reaction mixture.)

When the heavier PS-212 was used for the sacrificial layer, the liberation process with acetone yielded very tiny fragments of nanoparticle film (area < 0.5 mm<sup>2</sup>). Use of the lighter PS-7 yielded larger fragments (area < 5 mm<sup>2</sup>) of nanoparticle film after liberation with acetone. Similarly sized fragments were obtained for the nanoparticle film liberated from PLGA with acetone.

The work described to this point demonstrated that the SLED technique, as designed originally with a simple dissolve-the-polymer step, could liberate a multilayered nanoparticle film from the substrate on which it was first deposited. We believed, though, that we could further optimize the process to yield films with larger areas. In the next section, we describe how an

alternate chemistry for PLGA degradation could be harnessed to produce macroscopic nanoparticle film (area < 5 mm<sup>2</sup>).

### 5.5 Hydrolysis of PLGA to Yield Macroscopic Nanoparticle Films

One reason we selected PLGA to test as a sacrificial layer was that there is a second route by which to remove it. When exposed to water, PLGA is not dissolved directly, but instead is cleaved by hydrolysis of its ester linkages, reducing the polymer to its water-soluble monomers, lactic acid and glycolic acid [59]. Thus, the polymer constituents detaching from nanoparticle film are significantly smaller than the nanoparticles themselves. We anticipated that this approach, removing PLGA in water, would yield films larger than those produced by simply dissolving the polymer in acetone. Exposing the PLGA sacrificial layer to water yielded truly macroscopic nanoparticle films (Figure 5-5). These films could be transported to other substrates such as SU-8 scaffolds on silicon that we fabricated to support the films for imaging. Films of all dimensions could be inverted while in the water, allowing subsequent examination of the substrate-facing surface. Figure 5-6 shows nanoparticle film resting atop SU-8 scaffolds. The nanoparticle films have smooth edges and the iron oxide nanoparticles give rise to the brown hue of these films. Thin film interference and variations in the film thickness are responsible for their multicolored translucence.

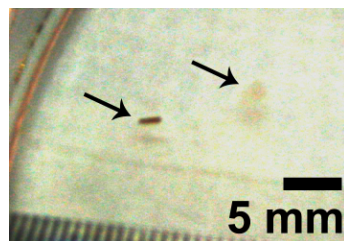


Figure 5-5. Photograph of iron oxide nanoparticle films floating on water after liberation, casting tinted shadows.

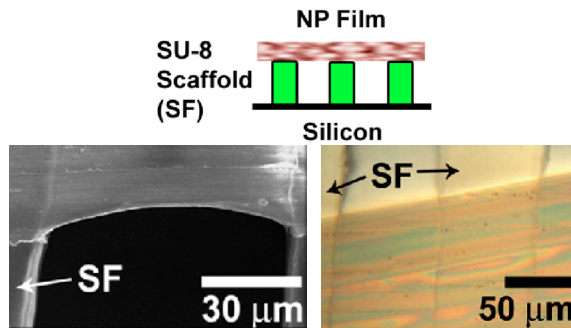


Figure 5-6. (Top) Diagram of nanoparticle film on SU-8 scaffold. (Left) SEM image of film on scaffold. (Right) Optical micrograph of film on scaffold.

After the nanoparticle films were released from the substrate, some PLGA could have remained on the films, bridging adjacent nanoparticles and helping to hold them together. A chemical analysis of the substrate-facing interface is insufficient to verify the complete removal of PLGA because the nanoparticles have their own organic coating, the ligands. Using AFM, we verified that PLGA was not acting to bind adjacent nanoparticles. Figure 5-7 presents representative AFM scans of the top and bottom surfaces, revealing well-delineated nanoparticle edges in both scans. An extant PLGA layer, spanning multiple nanoparticles, would have concealed these edges.

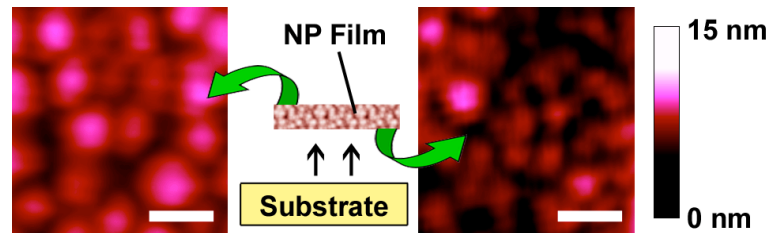


Figure 5-7. AFM images of top and bottom surfaces of NP film with discrete NPs visible, indicating removal of sacrificial polymer layer. The horizontal scale bars correspond to 30 nm.

The efficacy of PLGA as a sacrificial layer to release the nanoparticle film is facilitated by the polymer's interaction with water. An added benefit of using water is that the nanoparticle film is unperturbed since the hydrophobic end of oleic acid faces outward from the nanoparticles. In the context of the prior discussion on polymer size effects, the hydrolysis of PLGA to its

monomers is an ideal vehicle to facilitate nanoparticle film liberation. Because water is a poor solvent for the overall polymer chains, they do not expand readily and disrupt the film. Furthermore, the individual monomers that result from hydrolysis are notably smaller than the nanoparticles, and thus one monomer's motion is unlikely to disturb multiple nanoparticles.

### 5.6 Versatility of Sacrificial Layer Electrophoretic Deposition

Electrophoretic deposition enables the formation of multilayered films of a wide assortment of nanomaterials. Having demonstrated, using iron oxide nanoparticles, the capacity of the SLED technique to produce free-standing nanoparticle films that can be transferred to arbitrary substrates, e.g. SU-8 scaffolds, we explored the employment of this technique to produce films of other nanoparticles. Using cadmium selenide nanoparticles provided by Albert Dukes in the research group of Professor Sandra Rosenthal, we manually fashioned a doughnut-shaped section from a nanoparticle film that was transferred to a glass slide (Figure 5-8). The cadmium selenide nanoparticles were ~6.5 nm in total diameter, which included their dodecylphosphonic acid ligands. Thus, through the SLED technique, it is possible to obtain patternable, free-standing films comprising nanoparticles of differing composition, size, and ligand coating.

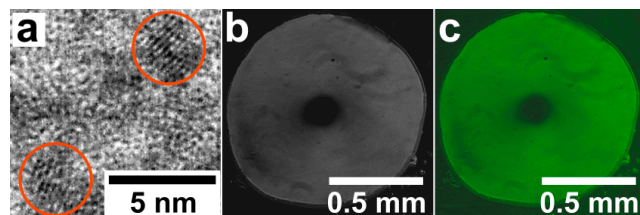


Figure 5-8. (a) TEM image of CdSe nanoparticles. Optical micrographs of CdSe nanoparticle film section on glass slide captured (b) without and (c) with fluorescent excitation.



Figure 5-9. Free-standing carbon nanotube films (buckypapers) produced by John Rigueur using the SLED technique. Figure provided by John Rigueur.

The range of application for SLED was expanded further in the Dickerson group by John Rigueur, who showed that it could be used to produce buckypapers, which are films comprising carbon nanotubes (Figure 5-9). The robustness of the SLED technique was demonstrated, in part, as the conditions for nanotube deposition (aqueous solvent, voltage < 10 V, current ~ 10 mA) differed greatly from the conditions for nanoparticle deposition (nonpolar solvent, voltage > 100 V, current ~ 100 nA). In this dissertation, we pursued the deposition of another low-dimensional carbon material suspended in water, graphene oxide, and the subsequent fabrication of its free-standing films. The next chapter details the synthesis and characterization of graphene oxide prior to its use in SLED experiments.